1up

NTIS HC $3.00

NASA TECHNICAL NOTE

NASA TN D-7156

NASA TN D-7156

SIMULTANEOUS FILM AND CONVECTION COOLING OF A PLATE INSERTED IN THE EXHAUST STREAM OF A GAS TURBINE COMBUSTOR

by Cecil J. Marek and Albert J. Juhasz

Lewis Research Center

Cleveland, Ohio 44135

NATIONAL AERONAUTICS AND SPACE ADMINISTRATION • WASHINGTON, D. C. • FEBRUARY 1973

1. Report No. NASA TN D-7156	2. Government Accession No.	3. Recipient's Catalog No.
4. Title and Subtitle SIMULTANEOUS FILM AND CONVECTION COOLING OF A PLATE INSERTED IN THE EXHAUST STREAM OF A GAS TURBINE COMBUSTOR		5. Report Date February 1973 6. Performing Organization Code
7. Author(s) Cecil J. Marek and Albert J. Juhasz		8. Performing Organization Report No. E-7165
9. Performing Organization Name and Address Lewis Research Center, National Aeronautics and Space Administration, Cleveland, Ohio 44135		10. Work Unit No. 501-24 11. Contract or Grant No.
12. Sponsoring Agency Name and Address National Aeronautics and Space Administration, Washington, D.C. 20546		13. Type of Report and Period Covered Technical Note 14. Sponsoring Agency Code
15. Supplementary Notes		

16. Abstract

Data were obtained on a parallel-flow film- and convection-cooled test section placed in the exhaust stream of a rectangular-sector combustor. The combustor was operated at atmospheric pressure and at exhaust temperatures of 589 and 1033 K (600° and 1400° F). The cooling air was at ambient pressure and temperature. Test results indicate that it is better to use combined film and convection cooling rather than either film or convection cooling alone for a fixed total coolant flow. An optimum ratio of film to convection cooling flow rates was determined for the particular geometry tested. The experimental results compared well with calculated results.

17. Key Words (Suggested by Author(s))	18. Distribution Statement
Liner cooling Combustors Film cooling	Unclassified - unlimited

19. Security Classif. (of this report)	20. Security Classif. (of this page)	21. No. of Pages	22. Price*
Unclassified	Unclassified	36	$3.00

*For sale by the National Technical Information Service, Springfield, Virginia 22151

CONTENTS

SIMULTANEOUS FILM AND CONVECTION COOLING OF A PLATE INSERTED IN THE EXHAUST STREAM OF A GAS TURBINE COMBUSTOR

by Cecil J. Marek and Albert J. Juhasz

Lewis Research Center

SUMMARY

Data were taken on a test section placed in the exhaust stream of a rectangular-sector combustor with film cooling alone, convection cooling alone, and simultaneous film and convection cooling. An optimum was found to exist for the ratio of film to convection cooling at a fixed total coolant flow for the parallel-flow, single-slot configuration. Simple expressions were derived to predict the optimum ratio when axial wall conduction was assumed to be small.

The experimental results were obtained at atmospheric pressure and combustor exhaust temperatures of 589 and 1033 K (600° and 1400° F). The cooling air was at ambient pressure and temperature. The wall temperatures were compared with calculated results. Good agreement was obtained for film cooling alone and convection cooling alone. The calculated results for combined film and convection cooling deviated as much as 30 percent from the experimental data. However, the calculated results showed the same trends as the experimental data. The turbulent-mixing coefficient C_m used in the turbulent-mixing film-cooling correlation was determined to be 0.03 in the combustor exhaust stream. This value was much lower than that previously found within the combustor.

INTRODUCTION

This investigation compares three methods of cooling a test wall exposed to a hot gas stream. The methods considered were film cooling alone, convection cooling alone, and simultaneous film and convection cooling. The study was motivated by the need to predict accurately combustor liner wall temperatures in advanced gas turbine engines. The high combustion chamber temperatures and pressures occurring in advanced engines necessitate that the cooling air be used as efficiently as possible. Insufficient cooling air would lead to liner damage, while excess cooling air would penalize the cycle efficiency and degrade the turbine-inlet temperature profile.

Conventional combustor liner design is based primarily on film cooling, with convection cooling occurring as a secondary mechanism in the process of ducting the film-cooling air to successive downstream slots. Based on an analytical derivation, Colladay (ref. 1) has shown that when film and convection cooling occur in series, it is beneficial to use as much of the available heat sink in the cooling air as possible for convection cooling before ejecting it as a film. To determine the improvement which might be obtained with more convection cooling than exists within conventional liners and to test the adequacy of available methods to predict the performance of the various cooling schemes, the following program was undertaken:

First, the desirability of using more convection cooling was investigated with the use of a double-walled test geometry.

Second, the turbulent-mixing correlation developed in reference 2 was evaluated for its capability to predict accurate temperatures of a film-cooled surface exposed to a combustor exhaust stream.

Finally, the validity of available predictive methods for the case of combined film and convective heat transfer was studied. Although methods have been developed which can be used in the analysis of combined film and convection cooling (refs. 1, and 3 to 5), they are generally applicable at distances far from the slot exit, where it may be assumed that the hot-gas convective-heat-transfer coefficient with film cooling is identical to the coefficient without film cooling.

In this work, data were taken on a 13-centimeter- (5.0-in.-) long, double-walled test section placed in the exhaust stream of a rectangular sector of a gas turbine combustor described in reference 6. The combustor was operated at atmospheric pressure and exhaust temperatures of 589 and 1033 K (600° and 1400° F). Hot-gas-to-cooling-air temperature differences, hot-gas velocities, and cooling flows were close to values existing in conventional gas turbine combustors. Hot-gas turbulence levels were assumed to be representative of the combustor exhaust stream. The experimental data were compared to analytical predictions, and an optimum ratio of film to convection cooling flow was shown to exist for a given geometry and combustor operating condition. Analytical expressions were derived for this optimum ratio.

ANALYSIS

Prediction of Wall Temperatures

The wall temperatures with simultaneous film and convection cooling are determined by solving the steady-state energy balance. The resulting equation at any distance x

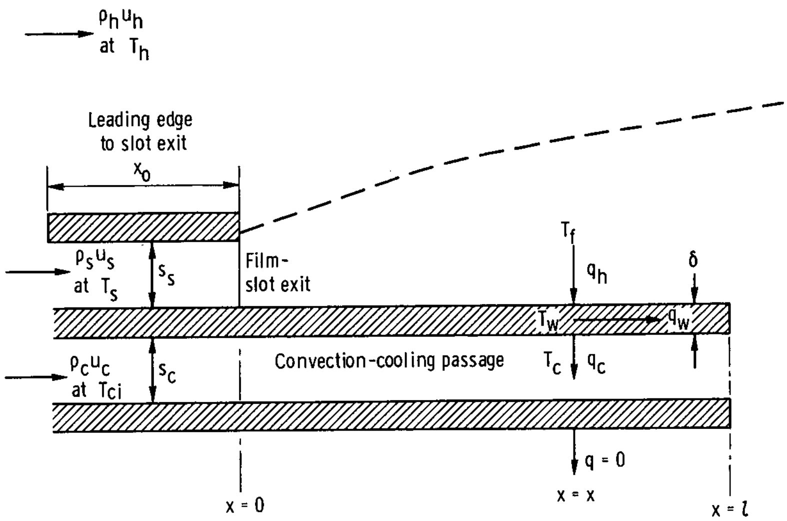

Figure 1. - Schematic for energy balance on wall.

downstream of the slot (see fig. 1) can be written as

$$\begin{pmatrix}\text{Net convection}\\ \text{to wall from}\\ \text{hot-gas side}\end{pmatrix} = \begin{pmatrix}\text{Net convection from}\\ \text{wall to cold}\\ \text{convection stream}\end{pmatrix} + \begin{pmatrix}\text{Net axial}\\ \text{conduction}\\ \text{along wall}\end{pmatrix}$$

or

$$q_h = q_c + q_w \tag{1}$$

The heat fluxes can be written in terms of the heat-transfer coefficients to obtain

$$h_h(T_f - T_w) = h_c(T_w - T_c) - k_w \delta \frac{d^2 T_w}{dx^2} \tag{2}$$

The effects of wall resistance and of radiation were neglected in equation (2), because they were insignificant at the test conditions considered herein. Axial conduction along the wall, however, has been included.

The turbulent-mixing correlation derived in reference 2 was used to calculate the film temperature. The turbulent-mixing correlation is

$$\eta_f = \frac{T_h - T_f}{T_h - T_s} = \frac{1}{1 + C_m \frac{x}{Ms_s}} \tag{3}$$

where C_m is the turbulent-mixing coefficient and M is the mass-flux ratio $\rho_s u_s/\rho_h u_h$. Equation (3) was used with and without convection to determine the film temperature T_f at any distance x downstream of the slot exit for a given value of C_m.

The hot-gas convective-heat-transfer coefficient h_h was calculated from the heat-transfer coefficient for a flat plate given by

$$h_h = 0.0365 \frac{k_h}{x + x_o} \left[\frac{(x + x_o)\rho_h u_h}{\mu_h}\right]^{0.8} (Pr_h)^{0.33} \tag{4}$$

The term x_o is the distance upstream of the slot exit, which is the apparent origin of the hot-gas turbulent boundary layer. Equation (4) was used with and without film cooling. The assumption that the heat-transfer coefficient depends only on the mainstream flow has been shown (refs. 3 to 5) to hold well far downstream of the slot exit at a distance greater than 70 slot heights. For discussion of the use of this equation in the near-slot region, refer to the RESULTS AND DISCUSSION section of this report.

The convection-cooling heat-transfer coefficient h_c was calculated from

$$h_c = 0.023 \frac{k_c}{2s_c} \left(\frac{2s_c \rho_c u_c}{\mu_c}\right)^{0.8} (Pr_c)^{0.33} \tag{5}$$

To determine the temperature of the convection stream T_c at any position x, equation (2) was solved simultaneously with the energy balance on the convection stream given by

$$s_c \rho_c u_c \left(C_p\right)_c \frac{dT_c}{dx} = h_c(T_w - T_c) \tag{6}$$

The boundary condition at $x = 0$ is that the cooling air and the wall temperature are equal. Thus, at $x = 0$

$$T_w = T_s \tag{7}$$

This condition was assumed because of the heat sink of the inlet tubes. The end of the wall, $x = l$, was assumed to be in contact with both the film and the convection streams. Thus, at $x = l$

$$k_w \frac{dT_w}{dx} = \frac{1}{2} h_h(T_f - T_w) + \frac{1}{2} h_c(T_c - T_w) \tag{8}$$

One-half the area of the exposed end has been arbitrarily assumed to be in contact with the film stream and one-half in contact with the convection stream.

Equations (2) and (6) were written in finite-difference form and solved by numerical iteration.

Optimization of Film to Convection Flows

A trade-off exists between film and convection cooling. The designer can adjust the film-cooling hole size or the convection passage height to deliver the flow at the optimum ratio.

The overall cooling effectiveness η_T can be related to the film- and convection-cooling effectiveness. The overall cooling effectiveness is

$$\eta_T \equiv \frac{T_h - T_w}{T_h - T_s} \tag{9}$$

The film-cooling effectiveness η_f is defined as

$$\eta_f \equiv \frac{T_h - T_f}{T_h - T_s} \tag{10}$$

and the convection-cooling effectiveness φ_c is defined as

$$\varphi_c \equiv \frac{T_f - T_w}{T_f - T_{ci}} \tag{11}$$

Then the overall cooling effectiveness for parallel-flow cooling where $T_s = T_{ci}$ is given by

$$\eta_T = \eta_f + \varphi_c - \eta_f \varphi_c \tag{12}$$

If the film-cooling effectiveness is very high, the change in the overall cooling effectiveness η_T with convection cooling is small, and conversely.

The convection-cooling effectiveness φ_c is related to the fraction of convection cooling Y_c when axial wall conduction is small by

$$\varphi_c = \frac{1}{1 + \frac{C_c}{Y_c}} \tag{13}$$

The coefficient C_c is given by

$$C_c \equiv \frac{\frac{St_h}{St_c} \frac{W_h}{W_T} \frac{A_c}{A_h} \frac{\left(C_p\right)_c}{\left(C_p\right)_h}}{1 - \frac{ax}{s_c} St_c} \tag{14}$$

where C_c is a function of geometry and hot-gas flow conditions and varies slightly with Y_c. The derivation of equations (13) to (17) is given in the appendix.

The film-cooling effectiveness can be written as

$$\eta_f = \frac{1}{1 + \frac{C_f}{Y_f}} \tag{15}$$

where C_f is given by

$$C_f \equiv \frac{C_m x}{s_s} \frac{W_h}{W_T} \frac{A_s}{A_h} \tag{16}$$

The overall cooling effectiveness, equation (12), can be maximized at a constant total coolant flow. The optimum ratio of film cooling to total cooling air for a fixed geometry and quantity of total cooling air (i.e., C_c and C_f are assumed to be constant) is given by

$$\left(Y_f\right)_{opt} = \frac{1 + C_c - C_f}{2} \tag{17}$$

When the difference between C_c and C_f is greater than 1, the optimum will be all film cooling or all convection cooling, depending on which coefficient is the greater.

The optimum ratio of film cooling to convection cooling is given by

$$\left(\frac{W_f}{W_c}\right)_{opt} = \frac{1 + C_c - C_f}{1 + C_f - C_c} \tag{18}$$

This relation can be used as a trial solution when making detailed calculations to search for the optimum under conditions where the assumptions of negligible axial wall conduction and radiation no longer hold.

APPARATUS AND INSTRUMENTATION

Flow System

The rectangular combustor test rig and associated airflow systems are shown schematically in figure 2. Ambient-temperature combustion airflow was measured by a square-edged orifice installed according to ASME standards. The air then entered a direct-fired preheater using ASTM-A1 fuel, where the temperature was increased to 589 K (600° F). A plenum chamber ensured a well-mixed flow at the test combustor inlet. The combustor exhaust entered the instrument section which housed eight five-point bare-wire platinum platinum-13-percent-rhodium thermocouples and seven five-point total pressure rakes for monitoring the combustor exhaust condition. The test section was installed in a windowed section downstream of the instrument section of the combustor.

Three independent cooling flows (convection air, film air, and slave air) were used to cool the test section. Film and convection air cooled the test surface, and slave air cooled the leading edge and undersurface of the test section. The three cooling flows were introduced separately and metered independently with standard ASME square-edged orificies. The combined combustor and cooling flow was finally exhausted through a water-quench scrubber to the atmosphere.

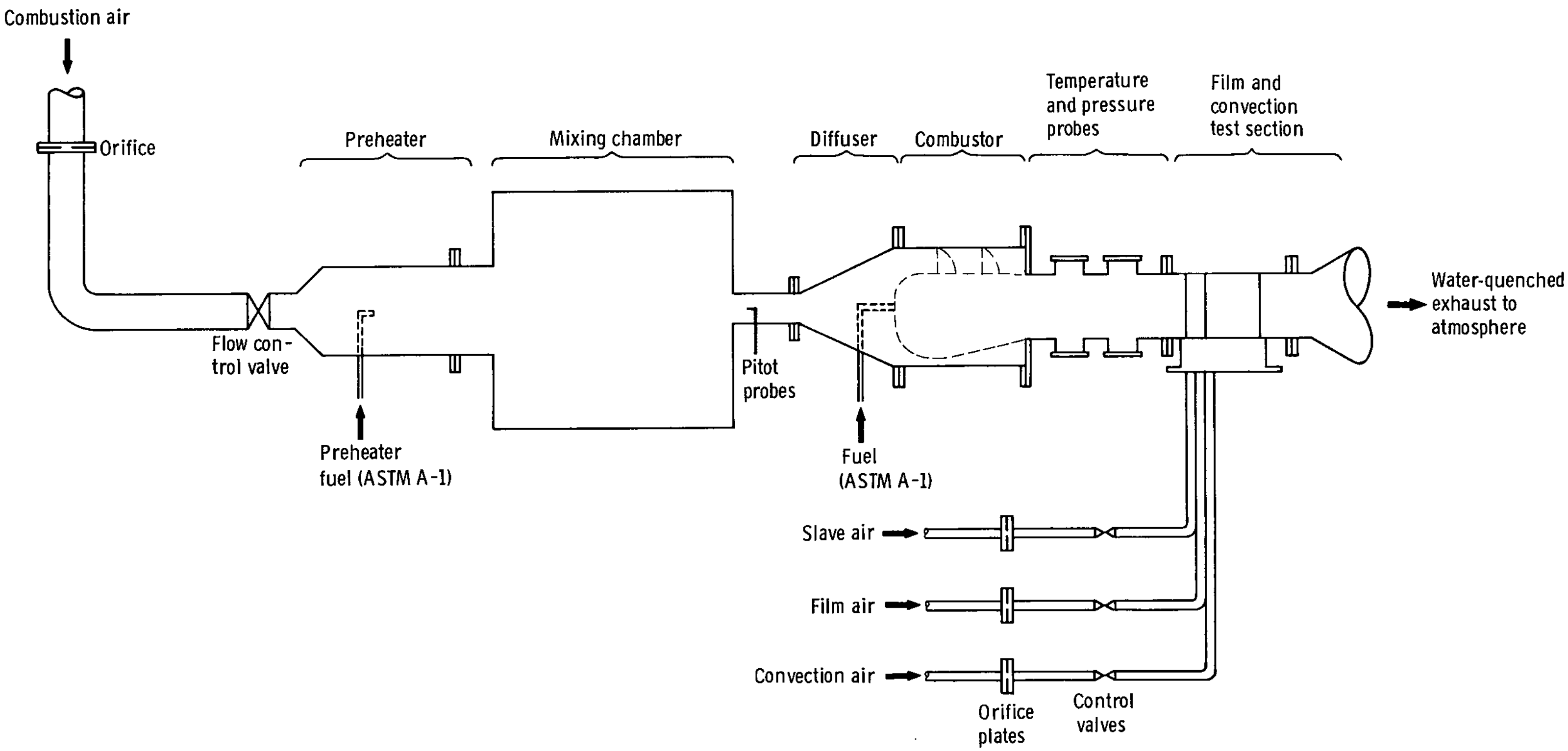

Figure 2. - Test setup-schematic of flow system.

Test Combustor

A rectangular one-side-entry type combustor was used to provide the hot gas stream for the cooling study. The design and performance of various side-entry type combustor models are reported in reference 6. The combustor was the same combustor used in the film-cooling study presented in reference 2, but with the film-cooling box removed. The combustor is shown schematically in figure 3, along with the location of the test section.

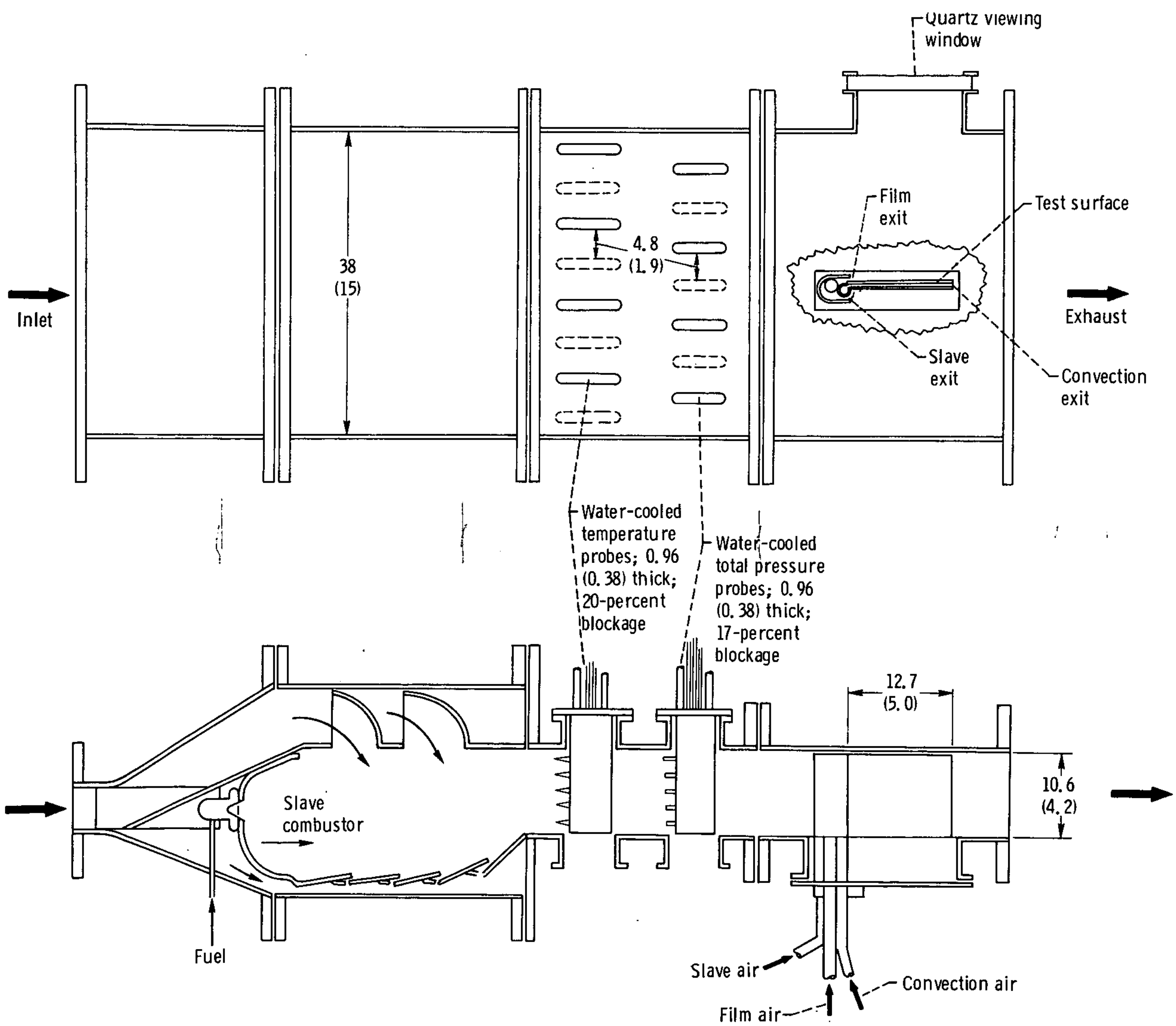

Figure 3. - Test combustor schematic showing location of combustor instrumentation and cooling test section. Dimensions are in cm (in.).

Test Section

The test surface was cooled by either film air, convection air, or simultaneous film and convection air. The slave air cooled the leading edge and undersurface by 222 K (400° F) but dropped the test surface temperature by, at most, 11 K (22° F) at the hot-gas condition of 1033 K (1400° F). No warpage of the test section was evident throughout the test program. All the air was brought through the side of the test section, as shown in figure 4. Flow distributors were inserted in the inlet tubes of the convection and film streams to give uniform flow across the test slot. Within the convection-air supply tube the flow distributor consisted of a smaller diameter tube with 10 holes 0.43 centimeter (0.187 in.) in diameter, with the holes at 180° from the slot exit. Within the film-cooling-air supply tube, the flow distributor was a semicylindrical rod with 15 holes 0.32 centimeter (0.125 in.) in diameter, which were drilled at right angles to the axis and also countersunk to provide for smooth turning of the flow. These inserts extended the complete length of the slot and resulted in a

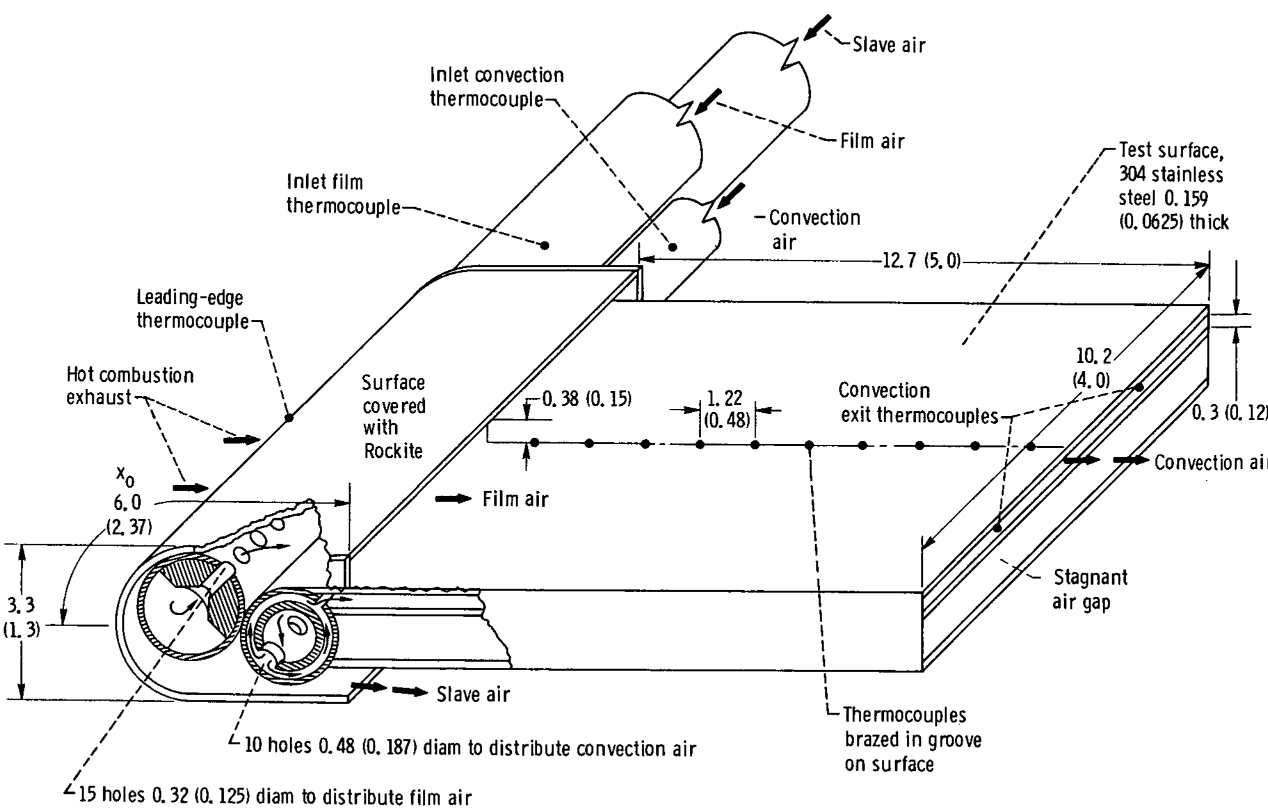

Figure 4. - Film- and convection-cooled test section showing location of the thermocouples and cooling inserts. Dimensions are in cm (in.).

center-peaked velocity profile, with the maximum velocity being about 20 percent above the mean.

The test surface was constructed of 0.159-centimeter- (0.0625-in.-) thick type-304 stainless steel. The leading edge and undersurface were 0.159-centimeter- (0.0625-in.-) thick Hastelloy.

The test surface was 10.2 centimeters (4.0 in.) wide by 12.7 centimeters (5.0 in.) long. The film-cooling slot exit was 0.38 centimeter (0.15 in.) high and the convection passage was 0.3 centimeter (0.12 in.) high.

The leading edge of the test section was flame sprayed with Rockite (an alumina oxide).

Temperature Instrumentation

Ten Chromel-Alumel (CA) thermocouples were installed 1.22 centimeters (0.48 in.) apart within grooves on the centerline of the test surface. The grooves were filled with filler braze to produce a smooth surface.

The inlet temperatures of the film and convection stream were measured with CA thermocouples inserted within the inlet tubes, as shown in figure 4. Because of failure of the film-cooling-inlet thermocouple early in the program, the film temperature was inferred by extrapolating the wall temperatures to the slot exit. A check of the film-inlet temperature was also provided by comparison to the convection-inlet temperature. The inlet temperatures were higher at low cooling flows because of conduction within the wall of the test section.

Two CA thermocouples were installed at the convection exit, and one CA thermocouple was placed on the leading edge of the test section.

The hot-gas temperature was determined by averaging the 10 platinum/platinum-13-percent-rhodium thermocouples on the two rakes above the test section in the combustor instrument section. Typical combustor exhaust temperatures at the 589 K (600° F) and the 1033 K (1400° F) conditions are shown in figure 5. The temperature parameter commonly used to describe a combustor exhaust stream is the pattern factor δ_p defined as

$$\delta_p = \frac{T_{\text{maximum exhaust}} - T_{\text{average exhaust}}}{T_{\text{average exhaust}} - T_{\text{combustor inlet}}} \tag{19}$$

The pattern factor for this combustor at the 1033 K (1400° F) condition was 0.33 and changed less than ± 0.01 over the range of combustor flow rates tested.

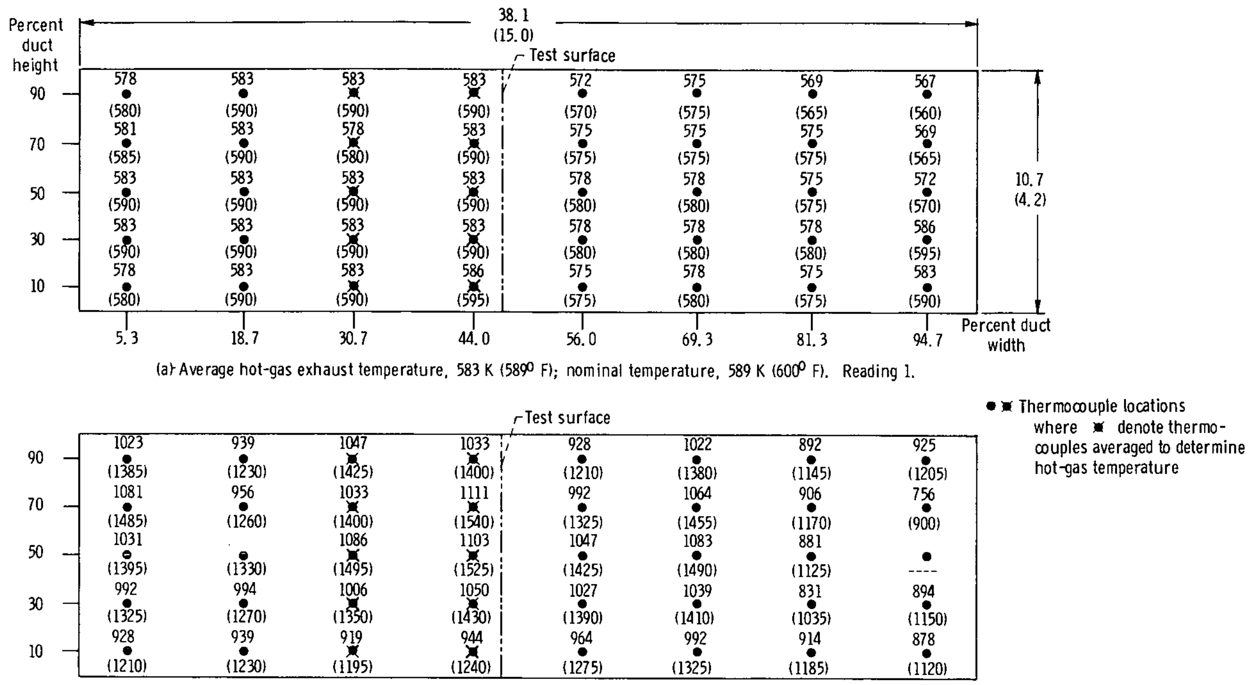

Figure 5. - Combustor exhaust temperatures in kelvin (°F). Location of temperatures in percentages of duct height and width. Dimensions in centimeters (in.). View looking downstream.

TEST CONDITIONS AND PROCEDURE

Range of Conditions

The combustor was operated at near atmospheric pressure throughout the test program. The combustor-inlet air temperature of 589 K (600° F) was provided by an upstream direct-fired heater. Combustor reference velocities were 20, 27, and 39 meters per second (64, 90, and 128 ft/sec). These reference velocities were computed from the airflow rate, the combustor-inlet static pressure and temperature, and the maximum cross-sectional area of the combustor housing (0.097 m^2, or 1.04 ft^2).

The cooling tests were performed at the four combustor operating conditions given in table I. Condition 1 was obtained without the main combustor burning, with only the preheater providing the temperature rise.

The cooling flows ranged from mass-flux ratios M of 0.4 to 4.4. The inlet coolant temperature ranged from 300 to 316 K (80° to 110° F).

TABLE I. - COMBUSTOR CONDITIONS

Condition	Combustor mass flow		Combustor exhaust temperature		Hot-gas velocity over test surface	
	kg/sec	lb/sec	K	^{o}F	m/sec	ft/sec
1	1.59	3.5	589	600	72	234
2	1.59	3.5	1033	1400	125	410
3	2.27	5.0	1033	1400	180	585
4	1.13	2.5	1033	1400	90	293

Estimated Accuracy of Temperatures

The hot-gas temperatures from the combustor were recorded for each cooling flow just prior to recording the test-surface temperatures. For the two rakes above the test section the maximum temperature varied from the average of the two rakes by as much as 100 K (180^{o} F) at the 1033 K (1400^{o} F) condition. The plate temperatures were reproducible to ±5 K (10^{o} F), but because of the drift of the combustor the overall accuracy of the test-surface temperatures was ±11 K (20^{o} F).

RESULTS AND DISCUSSION

Data were taken on a test section placed in the exhaust stream of a rectangular-sector combustor with film cooling alone, convection cooling alone, and simultaneous film and convection cooling.

The wall-temperature data are compared to the predicted wall temperatures calculated by the method described in the ANALYSIS section. Numerical finite-difference methods were used to solve the equations for all the tests. Correcting the wall temperatures for radiation amounted to less than a 2 percent change in the calculated wall temperatures. Hence, the effect of radiation was neglected in the calculations. Although the thermal conductivity of the wall ranged from 0.0081 to 0.013 J/sec-cm-K (8 to 13 Btu/hr-ft-^{o}F) over the temperature range from 311 to 811 K (100^{o} to 1000^{o} F), respectively, for type-304 stainless steel, a constant value of 0.01 J/sec-cm-K (10 Btu/hr-ft-^{o}F) was used for all the calculations.

The data are presented in terms of the reduced coolant flow, defined as the coolant flow per unit of cooled wall area over the hot-gas mass flux:

$$\text{Reduced coolant flow} = \begin{cases} \dfrac{\rho_c u_c s_c}{\rho_h u_h l} & \text{for convection cooling} \\ \\ \dfrac{\rho_s u_s s_s}{\rho_h u_h l} & \text{for film cooling} \end{cases}$$

The results of film cooling alone are discussed first, followed by the results of convection cooling alone and then by the results of simultaneous film and convection cooling. A complete listing of the experimental data is given in table II.

Film Cooling

Assuming the film temperature T_f to be equal to the measured wall temperature T_w at any x, the experimental film-cooling effectiveness was plotted as a function of the downstream distance parameter x/Ms_s, as shown in figure 6. The value of the turbulent-mixing coefficient C_m which best correlates the data was found to be 0.03. This is much lower than the value of 0.15 found within the same combustor (ref. 2), but is greater than the value of 0.01 found within low-turbulence wind tunnels. The value of C_m is considered to be lower in the exhaust stream than within the combustor because of the natural damping of turbulence which occurs with distance. Also, the turbulence was affected by the pressure and temperature rakes upstream of the test section. No attempt was made to measure the turbulence in the exhaust stream directly.

The agreement of the η-values predicted by the turbulent-mixing correlation (eq. (3)), with C_m equal to 0.03, was within 10 percent of the experimental data at

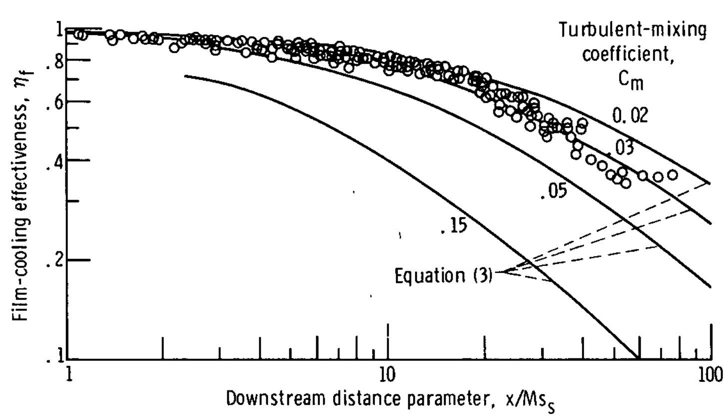

Figure 6. - Experimental film-cooling effectiveness as function of downstream distance parameter.

TABLE II. - EXPERIMENTAL DATA

(a) SI units

Run	Mass flow rate of hot gas, kg/sec	Hot-gas temperature, K	Mass flow rate of film, kg/sec	Reduced film flow rate	Inlet film temperature, K	Mass flow rate of convection, kg/sec	Reduced convection flow rate	Inlet convection temperature, K	Exit convection temperature, K	Wall temperatures, K, at specified downstream distances in centimeters									
										1.02	2.23	3.45	4.67	5.89	7.11	8.33	9.55	10.77	11.99
1	1.62	583	0.000	0.000	316	0.000	0.000	383	555	544	561	561	566	566	566	566	566	566	566
2	1.57	589	.018	.033	313			383	464	327	341	356	366	380	393	404	413	422	433
3	1.57	588	.036	.067	308			385	405	319	330	340	347	352	358	363	366	372	380
4	1.58	585	.050	.091	307			372	434	317	327	338	344	350	352	358	361	366	372
5	1.56	588	.068	.125	306			371	420	317	328	338	344	351	353	357	361	363	372
6	1.57	587	.057	.105	305	.000	.000	375	426	317	328	339	345	350	354	358	361	364	372
7		587	.050	.092	309			372	439	319	329	340	347	351	356	361	365	366	377
8		587	.018	.033	316			415	462	327	338	354	365	377	388	400	410	419	427
9		585	.036	.067	313			405	414	321	328	338	345	352	356	361	366	372	378
10		587	.027	.050	312			410	442	322	332	343	350	357	365	369	377	382	389
11	1.57	578	.023	.042	312	.000	.000	411	451	323	333	347	355	365	372	383	389	398	406
12	1.53	587	.009	.017	316	.000	.000	433	501	342	358	383	406	433	450	467	477	487	494
13	1.57	582	.014	.025	316	.000	.000	427	476	333	345	365	378	397	411	427	438	449	456
14	1.57	591	.000	.000	316	.000	.000	450	561	492	533	550	556	561	566	569	572	572	572
15	1.54	611	.000	.000	316	.009	.017	300	350	422	468	483	487	488	488	488	488	488	486
16	1.58	591	.000	.000	316	.018	.033	298	325	381	422	433	436	436	433	433	433	433	433
17	1.55	595	.000	.000	316	.036	.067	297	313	355	389	398	398	396	395	395	395	395	398
18	1.57	588	.000	.000	308	.057	.104	296	305	338	367	373	373	372	369	371	371	371	377
19	1.55	588	.000	.000	305	.092	.170	297	295	325	347	350	350	350	350	350	350	350	357
20	1.55	588	.036	.067	308	.000	.000	338	413	315	322	335	343	349	351	356	361	365	372
21	1.61	923	.052	.092	314	.000	.000	351	490	332	350	369	383	394	404	415	422	433	450
22	1.60	1143	.052	.093	316			382	534	346	366	394	411	427	438	455	466	476	500
23	1.58	1001	.035	.064	316			405	645	353	372	393	405	421	433	445	460	483	516
24	1.59	1045	.019	.034	316			444	741	377	400	434	466	504	538	577	616	652	677
25	1.57	1024	.010	.018	316			455	772	411	450	522	583	639	677	711	738	761	771
26	1.54	1016	.010	.018	316	.009	.017	310	358	338	355	405	456	505	538	566	583	594	600
27	1.59	1016	.010	.017	316	.018	.033	310	331	327	338	377	416	455	480	505	519	530	538
28	1.56	1024	.010	.018	316	.027	.049	305	330	326	334	367	405	438	456	478	493	501	511
29	1.59	1027	.019	.034	315	.027	.048	305	319	321	327	338	350	362	377	393	405	416	427
30	1.59	1043	.027	.049	307	.027	.049	304	316	317	326	337	344	353	360	367	373	382	388
31	1.59	1036	.027	.049	311	.018	.033	305	322	322	333	344	354	364	371	387	388	397	405
32		1037	.027	.049	316	.010	.018	306	333	327	338	354	366	378	388	400	411	421	427
33		1071	.027	.049	316	.000	.000	388	531	350	369	397	417	439	456	476	490	504	516
34		1029	.000	.000	316	.010	.017	306	382	617	715	728	732	735	740	744	744	745	738
35		1035	.000	.000	316	.019	.034	305	356	550	644	658	661	665	666	670	670	671	663
36	1.59	1044	.000	.000	316	.027	.049	305	341	504	594	605	607	607	607	607	607	607	605
37	2.27	1042	.027	.035	313	.028	.036	305	320	322	332	344	355	369	383	400	412	426	438
38	2.27	1025	.028	.036	316	.000	.000	394	543	360	383	415	443	475	500	527	548	566	574
39	2.27	1027	.018	.023	316	.000	.000	393	576	377	405	457	506	560	595	633	655	672	672
40	2.27	1027	.010	.012	316	.000	.000	395	620	432	515	626	687	728	750	767	777	777	767
41	2.27	1028	.036	.046	316	.000	.000	388	532	355	373	402	423	445	465	483	500	516	528
42	2.22	1033	.045	.059		.000	.000	384	527	351	371	399	416	434	447	462	473	486	505
43	2.27	1026	.054	.069		.000	.000	384	516	348	366	394	411	427	439	454	462	473	491
44	2.27	1025	.000	.000		.036	.046	306	340	500	602	610	611	611	611	611	611	611	605
45	2.22	1023	.000	.000		.027	.035	310	348	527	632	640	644	644	645	645	645	645	638
46	2.27	1021	.000	.000	316	.018	.023	310	365	573	682	693	698	700	705	707	707	707	696
47		1021	.000	.000	316	.009	.012	313	402	655	755	767	772	773	778	782	783	783	772
48		1023	.009	.012	305	.009	.012	314	361	360	464	566	615	651	666	683	693	692	691
49		1029	.009	.012	305	.018	.023	311	336	333	395	494	544	574	590	606	615	623	623
50		1034	.009	.012	305	.027	.035	309	327	323	368	455	500	527	547	556	566	573	577
51	2.27	1030	.018	.023	314	.027	.035	307	323	321	327	350	379	411	437	461	476	491	500
52	2.27	1030		.022	316	.018	.023	311	332	326	333	361	398	436	465	492	510	527	534
53	2.27	1015		.023	316	.009	.012	313	350	332	344	378	421	466	500	532	554	572	578
54	1.13	1038		.046	316	.009	.023	306	336	327	337	350	363	376	387	400	411	423	431
55	1.13	1018		.046	316	.000	.000	390	572	354	377	405	428	454	473	495	511	529	545
56	1.13	1009	.009	.023	316	.000	.000	390	597	372	402	450	494	540	576	610	632	644	648
57		1017	.027	.069		.000	.000	388	562	338	361	388	405	423	438	452	466	481	504
58		995	.000	.000		.027	.069	304	333	447	537	545	545	543	539	539	539	543	550
59		1007	.000	.000		.018	.046	304	360	494	598	612	613	612	611	611	611	611	611
60		1020	.000	.000		.009	.023	310	378	572	672	690	695	699	701	705	706	708	700
61	1.13	1005	.009	.023	315	.018	.046	304	320	320	325	343	366	395	416	438	454	468	476
62	1.13	1004	.014	.035	315	.014	.035	304	325	322	328	343	354	367	383	398	411	426	435

TABLE II. - Concluded. EXPERIMENTAL DATA

(b) U.S. customary units

Run	Mass flow rate of hot gas, lb/sec	Hot-gas temperature, °F	Mass flow rate of film, lb/sec	Reduced film flow rate	Inlet film temperature, °F	Mass flow rate of convection, lb/sec	Reduced convection flow rate	Inlet convection temperature, °F	Exit convection temperature, °F	Wall temperatures, °F, at specified downstream distances in inches									
										0.40	0.88	1.36	1.84	2.32	2.80	3.28	3.76	4.24	4.72
1	3.56	589	0.000	0.000	110	0.000	0.000	230	540	520	550	550	560	560	560	560	560	560	560
2	3.46	601	.040	.033	105			230	376	130	155	181	200	225	248	268	285	300	320
3	3.46	600	.080	.067	95			234	270	115	135	152	165	175	185	195	200	211	225
4	3.47	594	.110	.091	94			211	322	112	130	150	160	170	175	185	190	200	211
5	3.44	599	.150	.125	92			208	297	112	132	150	160	172	177	183	190	195	210
6	3.45	598	.126	.105	90	.000	.000	216	308	111	132	151	162	171	178	185	191	196	211
7	3.45	598	.110	.092	97			211	331	115	133	152	165	172	181	190	197	200	219
8	3.45	598	.040	.033	110			287	372	130	150	178	198	220	240	260	278	295	310
9	3.46	593	.080	.067	105			270	286	118	131	150	161	175	181	191	200	210	221
10	3.45	597	.060	.050	102			278	336	120	138	158	171	184	197	205	219	229	241
11	3.45	582	.050	.042	103	.000	.000	281	352	122	141	165	180	198	211	230	241	257	271
12	3.38	598	.020	.017	110	.000	.000	321	442	156	185	230	272	320	351	381	400	418	430
13	3.45	589	.030	.025	110	.000	.000	310	398	140	161	198	222	256	281	310	330	349	361
14	3.45	604	.000	.000	110	.000	.000	350	550	427	500	531	542	551	559	565	570	570	570
15	3.39	641	.000	.000	110	.020	.017	80	170	300	383	411	418	420	420	420	420	420	415
16	3.48	604	.000	.000	110	.040	.033	77	125	227	300	321	325	325	320	321	321	321	320
17	3.42	611	.000	.000	110	.080	.067	75	103	180	241	258	258	253	251	251	251	251	258
18	3.45	598	.000	.000	96	.125	.104	74	89	149	202	213	212	210	205	208	208	208	219
19	3.41	598	.000	.000	90	.202	.170	75	72	125	166	170	171	170	170	170	170	170	181
20	3.41	600	.080	.067	95	.000	.000	149	285	108	121	144	158	169	173	181	190	198	211
21	3.55	1201	.114	.092	106	.000	.000	172	423	138	170	205	230	250	268	288	301	320	350
22	3.52	1597	.114	.093	110			228	502	163	200	250	280	310	330	359	380	398	440
23	3.48	1342	.078	.064	110			270	702	177	210	248	270	298	320	341	368	410	470
24	3.50	1422	.041	.034	110			340	875	220	260	322	380	448	510	580	649	715	760
25	3.46	1384	.022	.018	110			360	930	280	350	480	590	691	760	821	870	910	928
26	3.40	1370	.021	.018	110	.020	.017	98	185	150	180	270	362	450	510	560	590	610	620
27	3.50	1370	.021	.017	110	.040	.033	98	136	130	150	220	290	359	405	449	475	495	509
28	3.43	1384	.021	.018	110	.059	.049	90	134	128	142	202	270	330	362	402	429	443	460
29	3.50	1390	.041	.034	107	.059	.048	90	115	118	129	150	170	192	220	248	270	290	310
30	3.51	1418	.060	.049	94	.060	.049	88	109	111	128	148	160	176	188	201	212	228	240
31	3.50	1406	.060	.049	100	.040	.033	90	120	120	140	160	178	196	209	238	240	256	270
32		1407	.060	.049	110	.022	.018	91	139	130	150	178	199	221	240	260	280	298	310
33		1468	.060	.049	110	.000	.000	240	497	170	205	255	292	331	362	398	422	448	470
34		1393	.000	.000	110	.021	.017	92	228	652	828	851	859	864	872	880	880	882	870
35		1403	.000	.000	110	.041	.034	90	182	530	700	725	730	738	740	747	747	748	735
36	3.50	1419	.000	.000	110	.060	.049	90	155	448	610	630	633	633	633	634	634	634	630
37	5.00	1416	.060	.035	104	.062	.036	90	117	121	138	160	180	205	230	260	282	308	330
38	5.00	1385	.062	.036	110	.000	.000	250	518	188	230	288	338	395	441	490	528	560	574
39	5.00	1390	.040	.023	110	.000	.000	249	577	220	270	363	451	548	611	680	720	750	750
40	5.00	1389	.021	.012	110	.000	.000	252	656	318	468	668	778	851	891	922	940	940	921
41	5.00	1391	.080	.046	110	.000	.000	240	499	180	213	265	302	342	378	411	440	469	492
42	4.90	1400	.100	.059		.000	.000	232	490	172	209	259	290	322	345	372	392	415	449
43	5.00	1387	.120	.069		.000	.000	232	469	168	200	250	281	310	331	358	372	393	425
44	5.00	1386	.000	.000		.080	.046	92	153	441	625	638	641	641	641	641	641	640	630
45	4.90	1382	.000	.000		.060	.035	98	167	490	679	692	700	700	702	702	702	702	690
46	5.00	1379	.000	.000	110	.040	.023	99	198	572	768	789	798	801	810	813	814	814	794
47		1378	.000	.000	110	.020	.012	104	264	720	900	921	930	932	941	949	950	950	930
48		1382	.020	.012	90	.020	.012	106	190	188	376	560	648	713	740	770	788	787	784
49		1392	.020	.012	90	.040	.023	100	146	140	252	430	520	574	602	631	648	662	662
50		1401	.020	.012	90	.060	.035	97	129	122	203	360	441	490	525	542	560	572	580
51	5.00	1395	.040	.023	106	.060	.035	94	122	118	130	170	223	280	327	370	398	425	441
52	5.00	1395	.039	.022	110	.040	.023	100	139	128	141	191	258	325	378	427	459	489	502
53	5.00	1367	.040	.023	110	.020	.012	104	171	139	160	222	298	380	440	498	538	570	582
54	2.50	1410	.040	.046	110	.020	.023	91	145	130	148	171	195	218	238	261	281	302	317
55	2.50	1372	.040	.046	110	.000	.000	242	570	178	220	270	312	358	393	431	460	493	522
56	2.50	1357	.020	.023	110	.000	.000	242	616	210	265	350	430	512	578	638	678	700	708
57		1372	.060	.069		.000	.000	240	553	150	190	240	270	303	329	355	379	407	448
58		1331	.000	.000		.060	.069	88	139	346	508	521	521	518	511	511	511	518	530
59		1353	.000	.000		.040	.046	86	188	430	618	643	644	642	640	640	640	640	640
60		1377	.000	.000		.020	.023	98	221	570	751	783	791	799	802	810	812	815	800
61	2.50	1349	.020	.023	107	.040	.046	88	117	116	125	159	200	251	290	330	358	383	398
62	2.50	1348	.030	.035	108	.030	.035	88	125	120	132	158	178	201	230	258	280	308	324

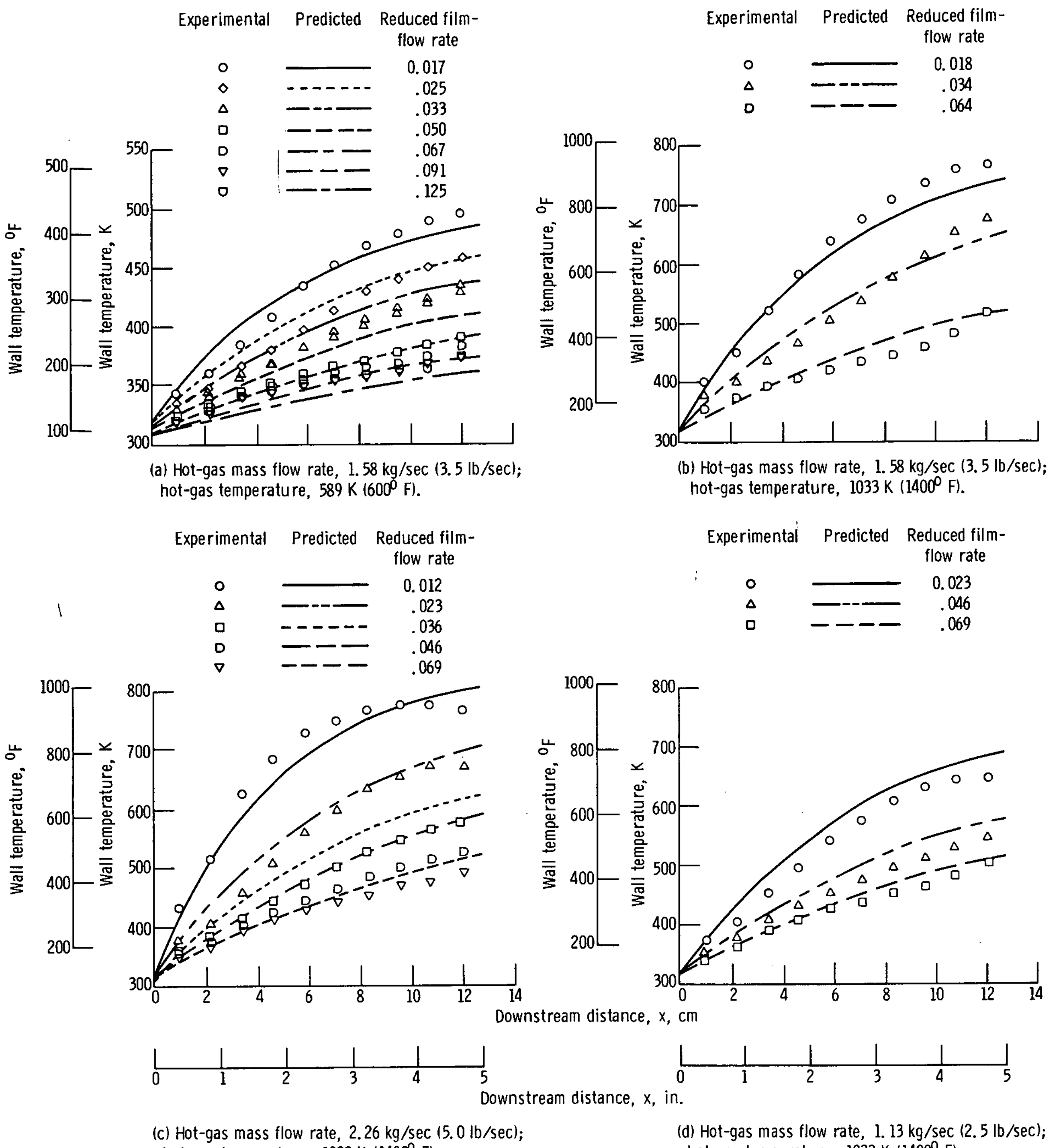

Figure 7. - Experimental and predicted wall temperatures for film cooling. Mixing coefficient C_m, 0.03; pressure, 1 atmosphere.

the four hot-gas conditions over the wide range of cooling flows tested.

The predicted wall temperatures are compared with experimental data in figure 7. The agreement between the predicted and experimental wall temperatures is good over the wide range of cooling flows, hot-gas flows, and hot-gas temperatures. However, there are deviations of ±25 percent evaluated in terms of the temperature difference between the wall and the inlet cooling air.

Axial wall conduction was included in the calculations; but the effect was small, resulting in less than a 4 percent change in the predicted wall temperatures. The axial conduction within the wall raised the inlet gas temperature by 11 K (20° F) at the high hot-gas temperatures and low cooling flows.

Convection Cooling

Figure 8 shows the experimental wall temperatures for convection cooling only and the calculated wall-temperature profiles predicted by five different methods. Except for a short distance close to the inlet, the experimental wall temperature was almost constant with increasing distance. This resulted from the ratio of the hot-gas to convection-

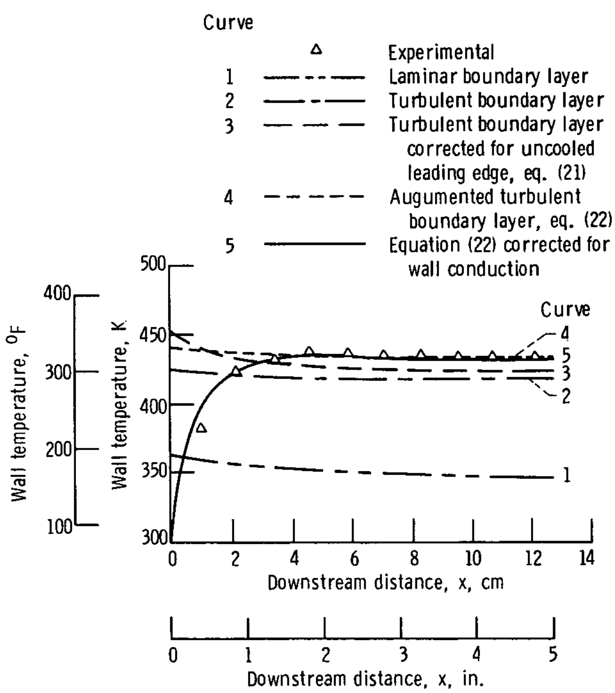

Figure 8. - Comparison of several hot-gas heat-transfer equations with experimental data for convection cooling. Hot-gas mass flow rate, 1.58 kg/sec (3.5 lb/sec); hot-gas temperature, 589 K (600° F); pressure, 1 atmosphere; reduced convection flow rate, 0.033.

cooling heat-transfer coefficients decreasing with distance as the hot-gas boundary layer develops. The decrease in this ratio would normally decrease the wall temperature; but since the convection-cooling temperature is increasing, the two effects compensate, producing a nearly constant wall temperature.

The Reynolds number at the slot exit based on the distance x_o from the stagnation point (6.02 cm or 2.37 in.) was 8.8×10^4. When the equation for a laminar boundary layer on a flat plate (curve 1) was used, the predicted wall temperatures were much lower than the experimental results. This was not surprising because of the high turbulence in the exhaust stream.

References 7 and 8 have shown that in a gas stream of high turbulence, transition from a laminar to turbulent boundary layer occurs at Reynolds numbers as low as 2×10^4. Based on the heat-transfer coefficient for turbulent flow on a flat plate, with the assumption that the origin of the thermal and hydrodynamic boundary layers occurs at the stagnation point, wall temperatures were obtained which were still too low (curve 2).

Since the leading edge was much hotter than the plate, a correction to the turbulent convective heat-transfer coefficient was made based on the assumption that the hydrodynamic boundary layer originated at the stagnation point but the thermal boundary layer originated at the slot exit. Tribus and Kline (ref. 9) have shown that with this correction the resulting hot-gas heat-transfer coefficient is given by

$$h_h = \frac{0.0292\, k_h}{\left[1 - \left(\dfrac{x_o}{x + x_o}\right)^{0.8}\right]^{0.11} (x + x_o)} \left[\frac{\rho_h u_h (x + x_o)}{\mu_h}\right]^{0.8} (Pr_h)^{0.33} \tag{21}$$

As shown by curve 3, the temperatures predicted by using equation (2) were slightly lower than the experimental results.

The best results were obtained by using a heat-transfer coefficient given by

$$h_h = \frac{0.0365\, k_h}{x + x_o} \left[\frac{\rho_h u_h (x + x_o)}{\mu_h}\right]^{0.8} (Pr_h)^{0.33} \tag{22}$$

The increase in hot-gas heat-transfer coefficient over that predicted by equation (21) was probably caused by the step in the wall for the film-cooling-slot exit producing separation of the hot-gas stream and reattachment to the wall downstream of the slot exit. Equation (22) (curve 4) resulted in good agreement with the experimental temperatures except for those measured in the vicinity of the slot exit. Curve 5 shows that

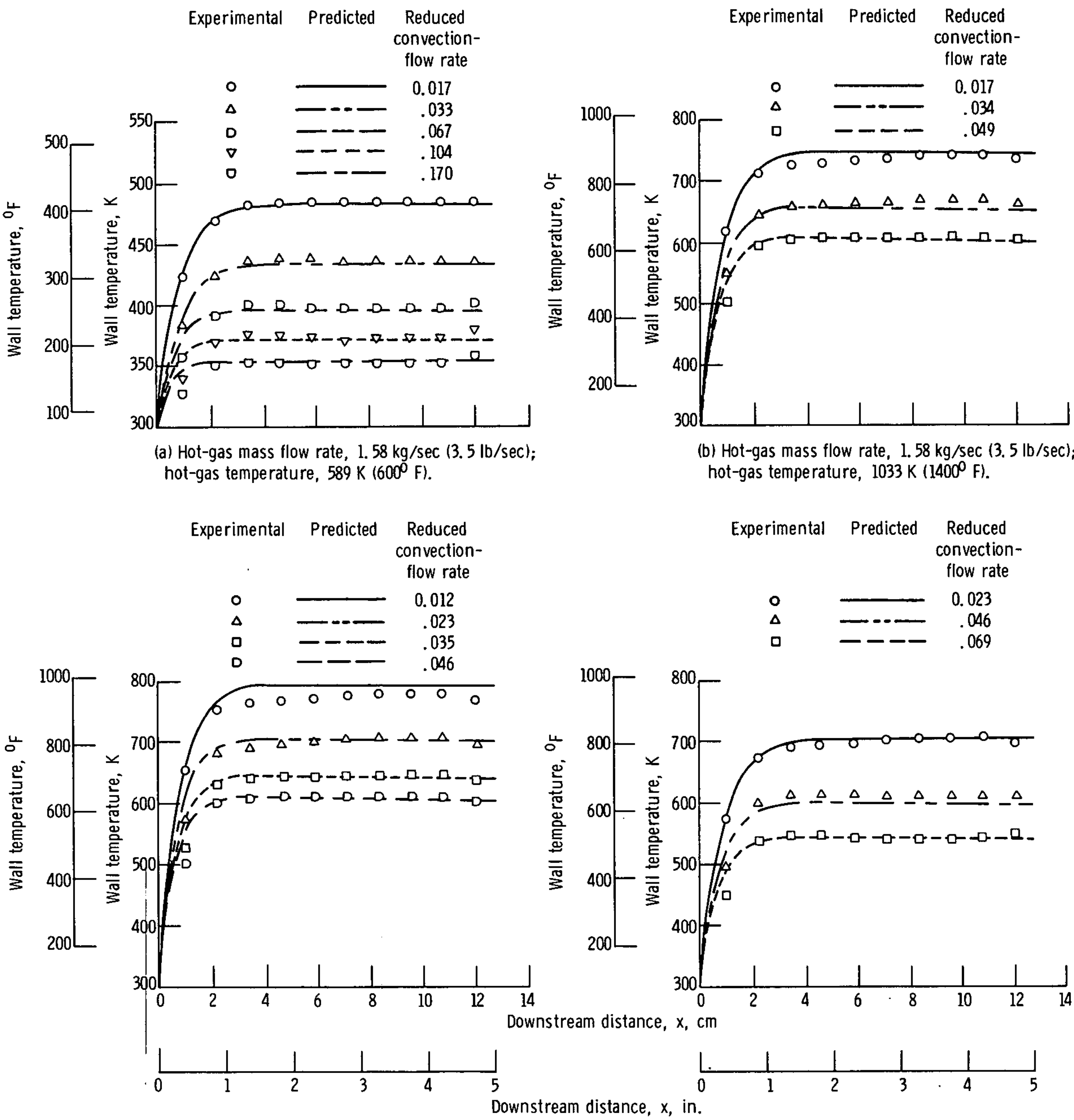

(a) Hot-gas mass flow rate, 1.58 kg/sec (3.5 lb/sec); hot-gas temperature, 589 K (600° F).

(b) Hot-gas mass flow rate, 1.58 kg/sec (3.5 lb/sec); hot-gas temperature, 1033 K (1400° F).

(c) Hot-gas mass flow rate, 2.26 kg/sec (5.0 lb/sec); hot-gas temperature, 1033 K (1400° F).

(d) Hot-gas mass flow rate, 1.13 kg/sec (2.5 lb/sec); hot-gas temperature, 1033 K (1400° F).

Figure 9. - Experimental and predicted wall temperatures for convection cooling. Pressure, 1 atmosphere.

correcting the wall temperatures for axial conduction, because of the sink effect of the inlet tubes, resulted in good agreement with the experimental temperatures for the entire length of the plate. In this experiment, conduction effects were apparent 3.8 centimeters (1.5 in.) from the slot exit.

Using equation (22) resulted in good agreement for the other hot-gas conditions and cooling flows, as shown in figure 9. The predicted wall temperatures agreed with the experimental data within 5 percent.

Simultaneous Film and Convection Cooling

In this section the trade-off between film and convection cooling is discussed.

Figure 10 shows the comparison of the predicted results and the experimental data, when the film flow rate was held constant and the rate of convection cooling was increased. Increasing the convective cooling rate does significantly lower the wall temperatures, as expected.

The agreement between the predicted results and the experimental data is not as

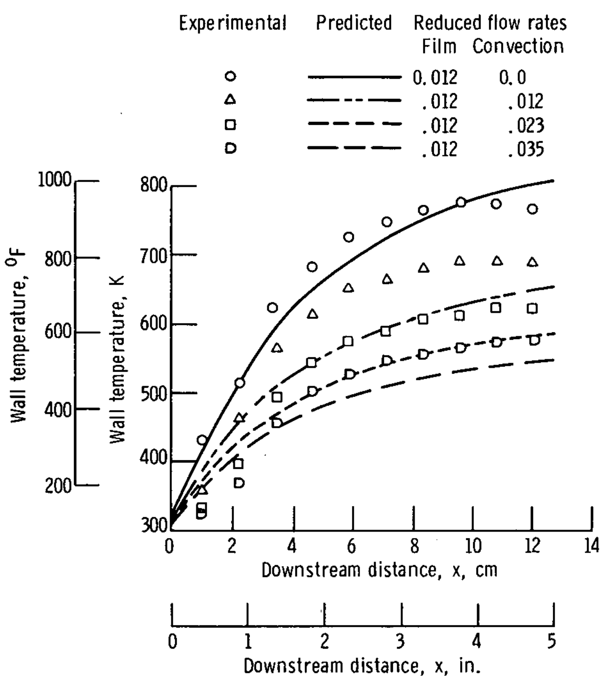

Figure 10. - Experimental and predicted wall temperatures for combined film and convection cooling for constant film-cooling flow rate of 0.0091 kg/sec (0.02 lb/sec) with increasing convection cooling. Hot-gas mass flow rate, 2.26 kg/sec (5.0 lb/sec); nominal hot-gas temperature, 1033 K (1400° F); pressure, 1 atmosphere.

good as with film or convection cooling alone. The assumption used here was that the heat-transfer coefficient on the hot-gas side is independent of the film flow rate. It is evident that the hot-gas-side heat-transfer coefficient did change with film flow rate. Except for the region in the vicinity of the slot, the correlation underpredicted the wall temperatures obtained by as much as 80 K (140° F). This may be caused by the hot-side heat-transfer coefficient changing with film flow rate. Seban (ref. 3) shows that at x/s_s values greater than 70, the predicted and experimental wall temperatures will again agree, suggesting that at larger distances from the slot exit the hot-gas flow field is independent of the film flow rate. In this experiment the maximum x/s_s at the downstream end of the test section was 33. Therefore, one would expect that the hot-gas convective coefficient would be affected by the film flow. No attempt was made to adjust the heat-transfer-coefficient expressions because of the complicated flow field, present on the hot-gas side, resulting from the film-cooling jet streams from the tube inserts spreading out on the slot lip and interacting with the hot-gas stream.

Figures 11(a) to (c) demonstrate the trade-off between film and convection cooling. In each figure the total amount of cooling flow was held constant. An optimum exists for the ratio of film to convection cooling which results in a minimum wall temperature with a fixed quantity of total cooling air. A wall-temperature reduction of as much as 69 K (125° F) results, compared to the all-film case, by using a film to convection coolant flow ratio of near 1. One explanation for the lower temperatures obtained with combined film and convection cooling is that the cooling air is in contact with both sides of the wall, increasing the effective area for heat transfer from the wall. With either cooling mode alone, the cooling air sweeps one side of the wall only. Therefore, at the optimum conditions both forms of cooling usually exist.

The predicted data do not show as large an effect as observed experimentally, but the same trends are indicated. The deviation between the experimental and the predicted results is as much as 30 percent.

The use of the equations derived for predicting the effect of cooling flow rate on the cooling effectiveness is presented in figure 12. With this geometry at a reduced cooling flow of 0.069, $C_f = 0.416$, and $C_c = 0.512$ so that the optimum predicted by equation (17) is 0.548. The agreement between the actual and the predicted optimum is fair. The curve is relatively flat at the optimum so that a slight deviation from the optimum ratio does not change the overall cooling effectiveness greatly. Although the advantage appears small over either all-film or all-convection cooling, an improvement of 0.1 in the cooling effectiveness may represent a change of 111 K (200° F), which could significantly improve the life of the liner.

The optimum ratio of film-cooling flow rate to convection-cooling flow rate at other reduced total cooling flows can be obtained by using equations (14), (16), and (17). The parameter C_f is inversely proportional to the reduced total cooling flow, while C_c

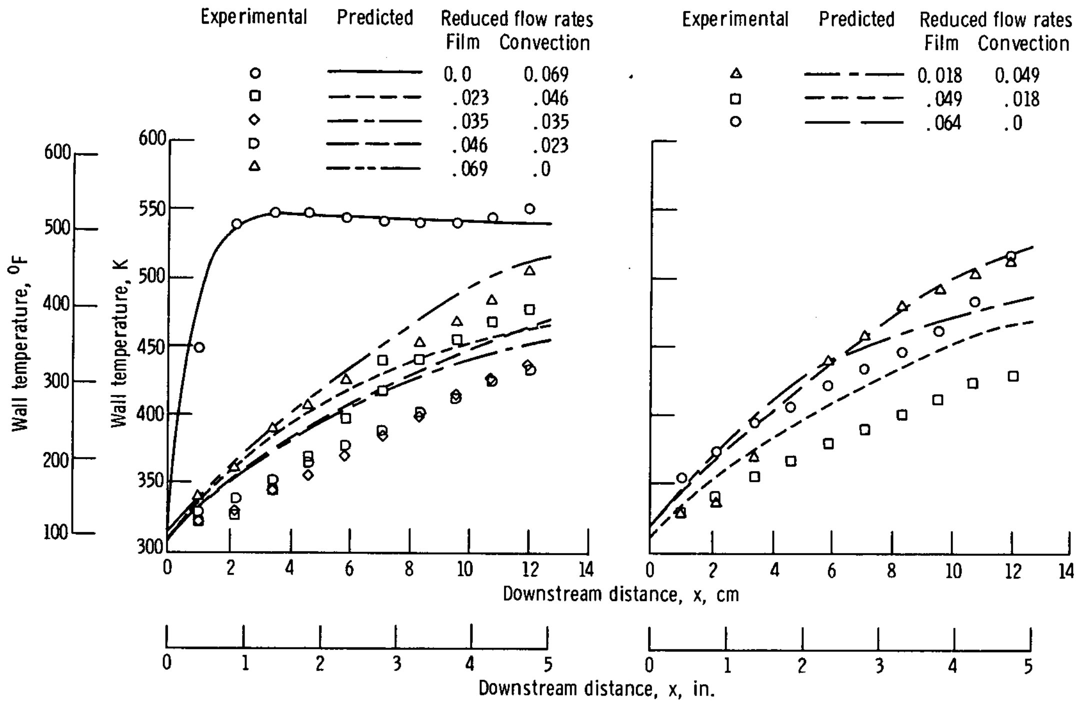

(a) Hot-gas mass flow rate, 1.13 kg/sec (2.5 lb/sec); total cooling mass flow rate, 0.027 kg/sec (0.06 lb/sec).

(b) Hot-gas mass flow rate, 1.58 kg/sec (3.5 lb/sec); total cooling mass flow rate, 0.0361 kg/sec (0.08 lb/sec).

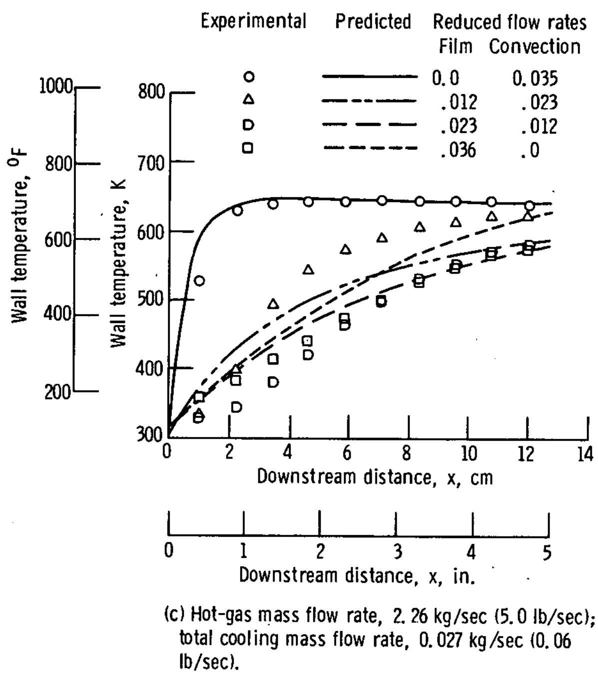

(c) Hot-gas mass flow rate, 2.26 kg/sec (5.0 lb/sec); total cooling mass flow rate, 0.027 kg/sec (0.06 lb/sec).

Figure 11. - Experimental and predicted wall temperatures for combined film and convection cooling showing the effect of the trade-off between film and convection cooling. Hot-gas temperature, 1033 K (1400° F); pressure, 1 atmosphere.

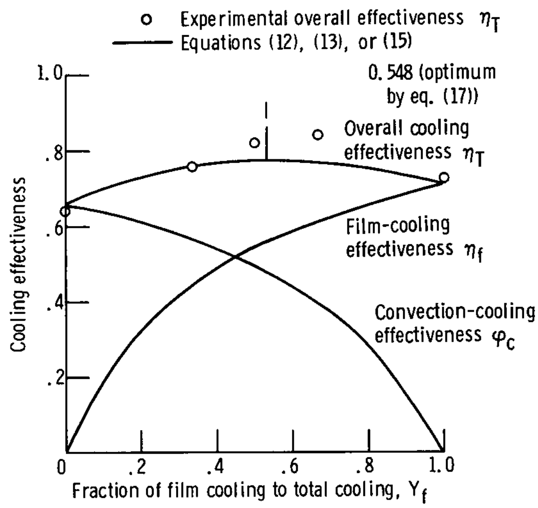

Figure 12. - Experimental and predicted cooling effectiveness as function of film-flow fraction. Downstream distance, 12.2 cm (4.8 in.); hot-gas mass flow rate, 1.13 kg/sec (2.5 lb/sec); hot-gas temperature, 1033 K (1400° F); pressure, 1 atmosphere; total cooling mass flow rate, 0.027 kg/sec (0.06 lb/sec).

varies inversely as the 0.8 power of the reduced total cooling flow. Over the conditions shown in figure 11, the optimum ratio of film-cooling flow rate to total cooling remains nearly constant at 0.548.

The magnitudes of C_f and C_c can be determined by doing calculations with film cooling alone and convection cooling alone. In this case Y_f and Y_c equal 1 and the overall cooling effectiveness will be equal to the film- and convection-cooling effectiveness, respectively. Therefore, as with the present test section, if the wall temperature is cooler with film cooling alone than with convection cooling, C_f is smaller than C_c and the optimum will be towards more film cooling than convection cooling.

Several additional results can be derived from equations (14), (16), and (17). As the convection-cooling effectiveness is raised by using a higher pressure drop or extended surfaces, the optimum ratio of film to convection cooling shifts towards more convection cooling.

The film-cooling coefficient C_f increases directly with downstream distance, whereas the convection-cooling coefficient C_c varies slightly with distance so that for short walls more film cooling should be used than convection cooling. For long walls the ratio shifts toward more convection cooling.

In general, an optimum usually exists for a single slot in the film- to convection-cooling ratio; and significant improvement may be attained by cooling the wall with the optimum ratio of film to convection cooling.

Applications

The analysis and experimental results show that, for a single slot in parallel flow, it is better to use combined film and convection cooling and that an optimum ratio of film to convection cooling exists. At this optimum ratio, a maximum cooling effectiveness at a given total cooling airflow will be obtained. In order to remove the heat efficiently, the flow passages should be designed to deliver the film and convection streams at the optimum cooling flow ratio. The optimum ratio depends on whether the convection or film stream is more effective in cooling the wall. If convection is more effective for a particular geometry, the optimum cooling flow ratio will be toward more convection cooling, and conversely. In general, it is better to use both forms of cooling.

Using all the air in a counterflow scheme to first convectively cool and then film cool will result in still a higher cooling effectiveness (ref. 1). The trade-off between parallel-flow and counterflow cooling needs to be determined for the individual case in terms of available passage space and allowable pressure drop. For the same passage heights the counterflow geometry would require additional pressure drop.

For a multiple-segmented liner, the analysis presented in this report would apply to the first section. The decision to introduce fresh film flow to the second slot, as shown in figure 13(a), or to pass the air through the convection passage as in figure 13(b) needs to be determined in terms of the allowable pressure drop and the temperature rise of the convective stream.

At the higher temperatures and mass fluxes in advanced gas turbines, the cooling air can be used more effectively if the convective-cooling heat transfer is increased by such means as utilizing a double-walled liner or using fins where sufficient pressure drop is available.

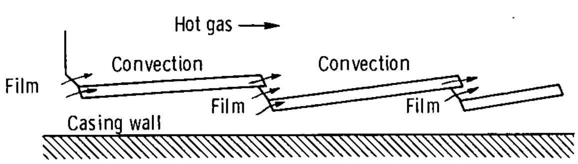

(a) Fresh film air introduced after first segment.

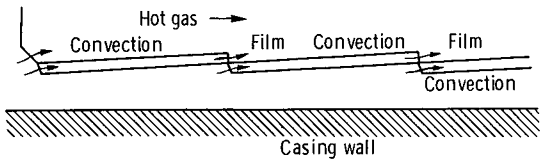

(b) No fresh film air introduced after first segment.

Figure 13. - Two alternates in design of multiple segmented liners.

SUMMARY OF RESULTS

Film and convection cooling data were taken on a parallel-flow test section installed in the exhaust stream of a combustor. The following results were obtained:

1. An optimum in the ratio of film and convection cooling flows was shown to exist. The optimum is dependent on the particular geometry and the total reduced coolant flow.

2. A simple expression was derived for the optimum film to convection coolant flow ratio when the axial wall conduction was negligible.

3. The turbulent-mixing film-cooling correlation worked well over a range of exit gas temperatures and exhaust gas flows with a turbulent-mixing coefficient C_m of 0.03. The value of 0.03 for C_m in the exhaust stream was considerably lower than within the same combustor, where C_m was equal to 0.15.

4. The predicted wall temperatures with convection cooling alone agreed well with experimental values when an adjusted hot-gas heat-transfer coefficient for a flat plate was used.

5. The prediction of wall temperatures with simultaneous film and convection cooling using the hot-gas heat-transfer coefficient without film cooling showed deviations from the experimental values in the near-slot region. However, the effect of the film to convection coolant flow ratio on the predicted wall temperatures showed the same trends as the experimental data.

Lewis Research Center,
National Aeronautics and Space Administration,
Cleveland, Ohio, October 17, 1972,
501-24.

APPENDIX A

DERIVATION OF OPTIMUM RATIO OF FILM TO CONVECTION COOLING FLOWS

The basic equations for predicting the wall temperatures have been presented in the ANALYSIS section. The optimum ratio of film to convection cooling flow will be derived for the case of thin walls where the wall resistance and axial wall conduction is negligible.

Effect of Convective Coolant Mass Flow Rate

For a wall of unit depth, the wall temperature is related to the heat-transfer coefficients by

$$h_h(T_f - T_w) = h_c(T_w - T_c) \tag{A1}$$

or

$$\frac{T_f - T_w}{T_w - T_c} = \frac{St_c}{St_h} \frac{W_c}{W_h} \frac{A_h}{A_c} \frac{\left(C_p\right)_h}{\left(C_p\right)_c} \tag{A2}$$

where St_c and St_h are the Stanton numbers for the coolant and hot gas, respectively. The Stanton number is defined as

$$St \equiv \frac{h}{\rho u C_p} \tag{A3}$$

and for the coolant is given by

$$St_c \equiv \frac{h_c}{\rho_c u_c C_p} = \frac{0.023}{(Re_c)^{0.2}(Pr_c)^{0.66}} \tag{A4}$$

Doubling the flow will decrease the Stanton number by only 13 percent, so for the purposes of the optimization it will be considered to be constant.

The convective-cooling effectiveness φ_c must be related to the convective coolant flow for a given film-cooling flow rate. The desired relation is obtained through the convective energy balance or

$$\rho_c u_c \left(C_p\right)_c s_c \frac{dT_c}{dx} = h_c(T_w - T_c) \tag{A5}$$

or

$$\frac{T_c - T_{ci}}{T_w - T_{ci}} = St_c \frac{x}{s_c} a \tag{A6}$$

where a is the mean effective temperature difference, defined as

$$a \equiv \frac{1}{T_w - T_{ci}} \frac{1}{x} \int_0^x (T_w - T_c)\, dx \tag{A7}$$

The value of a is unity at the slot exit and decreases with increasing distance. From equations (A2) and (A6), an expression for the overall convective-cooling effectiveness φ_c is given by

$$\varphi_c = \frac{T_f - T_w}{T_f - T_{ci}} = \frac{1}{1 + \dfrac{\dfrac{St_h}{St_c} \dfrac{W_h}{W_c} \dfrac{A_c}{A_h} \dfrac{\left(C_p\right)_c}{\left(C_p\right)_h}}{1 - \dfrac{ax}{s_c} St_c}} \tag{A8}$$

$$= \frac{1}{1 + \dfrac{C_c}{Y_c}} \tag{A9}$$

where Y_c is the fraction of convection air to total cooling air and C_c is defined as

$$C_c \equiv \frac{\dfrac{St_h}{St_c}\,\dfrac{W_h}{W_T}\,\dfrac{A_c}{A_h}\,\dfrac{\left(C_p\right)_c}{\left(C_p\right)_h}}{1 - \dfrac{ax}{s_c}\,St_c} \tag{A10}$$

where C_c is a mild function of the convective coolant flow but for the optimization will be considered constant.

Effect of Film Coolant Mass Flow Rate

The turbulent-mixing film-cooling correlation will be used here to express the relation between the film coolant flow rate and the film temperature

$$\eta_f \equiv \frac{T_h - T_f}{T_h - T_s} = \frac{1}{1 + \dfrac{C_m x}{M s_s}} \tag{A11}$$

$$= \frac{1}{1 + \dfrac{C_f}{Y_f}} \tag{A12}$$

where Y_f is the mass ratio of film flow to total flow and C_f is defined as

$$C_f \equiv \frac{C_m x}{s_s}\,\frac{W_h}{W_T}\,\frac{A_s}{A_h} \tag{A13}$$

Here C_f is constant and independent of the convection to film coolant flow split.

Optimization of Ratio of Film to Convection Coolant Flow Rates

The overall effectiveness for parallel-flow cooling where the initial film and convection temperatures are equal is given by

$$\eta_T \equiv \frac{T_h - T_w}{T_h - T_{ci}} = \eta_f + \varphi_c - \eta_f \varphi_c \tag{A14}$$

Now η_T can be maximized by using equations (A9) and (A12); holding the hot-gas condition, total coolant flow, and downstream distance x constant; and remembering that

$$Y_c + Y_f = 1 \tag{A15}$$

By using the method of Lagrangian multipliers we obtain the optimum condition

$$\frac{Y_c}{\varphi_c} = \frac{Y_f}{\eta_f} \tag{A16}$$

This relation will hold at the optimum condition. Several other forms exist for this relation which can be obtained by rearranging equations (A9), (A12), and (A14). For a known total coolant rate and geometry

$$\left(Y_c\right)_{opt} = \frac{1 + C_f - C_c}{2} \tag{A17}$$

and

$$\left(Y_f\right)_{opt} = \frac{1 + C_c - C_f}{2} \tag{A18}$$

For a known η_T which we desire to achieve we have

$$\left(\varphi_c\right)_{opt} = 1 - \sqrt{\frac{C_c}{C_f}(1 - \eta_T)} \tag{A19}$$

$$\left(\eta_f\right)_{opt} = 1 - \sqrt{\frac{C_f}{C_c}(1 - \eta_T)} \tag{A20}$$

where the ratio of C_f/C_c will not vary significantly with the total coolant flow.

Where radiation and axial wall conduction are important, these relations can be used as first approximations; but detailed calculations must be done for the particular geometry.

APPENDIX B

SYMBOLS

A	area
a	reduced mean driving force, defined by eq. (A7)
C_c	parameter defined by eq. (14)
C_f	parameter defined by eq. (16)
C_m	turbulent-mixing coefficient
C_p	specific heat
h	heat-transfer coefficient
k	thermal conductivity
l	length of test surface
M	mass-flux ratio, $\rho_s u_s / \rho_h u_h$
Pr	Prandtl number
q	heat flux
Re	Reynolds number
St	Stanton number
s_c	convection passage height
s_s	film slot height
T_c	convection temperature
T_{ci}	convection-inlet temperature
T_f	film temperature
T_h	hot-gas temperature
T_s	film-inlet temperature
T_w	wall temperature
u	velocity
W	mass flow rate
W_T	total cooling flow rate, film plus convection
x	distance downstream of slot exit

x_o leading edge upstream of slot exit

Y mass fraction of film- or convection-cooling flow to total cooling flow

δ wall thickness of test section

δ_p combustor exhaust pattern factor

η_f film-cooling effectiveness, defined by eq. (10)

η_T overall cooling effectiveness, defined by eq. (9)

μ viscosity

ρ mass density

φ_c convection-cooling effectiveness, defined by eq. (11)

Subscripts:

c convection conditions

f film conditions

h hot-gas conditions

opt conditions at optimum ratio of film to convection cooling

s film slot exit conditions

w wall properties

REFERENCES

1. Colladay, Raymond S.: Analysis and Comparison of Wall Cooling Schemes for Advanced Gas Turbine Applications. NASA TN D-6633, 1972.

2. Juhasz, Albert J.; and Marek, Cecil J.: Combustor Liner Film Cooling in the Presence of High Free-Stream Turbulence. NASA TN D-6360, 1971.

3. Seban, R. A.: Heat Transfer and Effectiveness for a Turbulent Boundary Layer with Tangential Fluid Injection. J. Heat Transfer, vol. 82, no. 4, Nov. 1960, pp. 303-312.

4. Hartnett, J. P.; Birkebak, R. C.; and Eckert, E. R. G.: Velocity Distributions, Temperature Distributions, Effectiveness and Heat Transfer for Air Injected Through a Tangential Slot into a Turbulent Boundary Layer. J. Heat Transfer, vol. 83, no. 3, Aug. 1961, pp. 293-306.

5. Eriksen, V. L.: Film Cooling Effectiveness and Heat Transfer with Injection through Holes. Rep. HTL-TR-102, Minnesota Univ. (NASA CR-72991), Aug. 1971.

6. Humenik, Francis M.: Performance of Short Length Turbojet Combustor Insensitive to Radial Distortion of Inlet Airflow. NASA TN D-5570, 1970.

7. Arici, Oener: Effects of Free-Stream Turbulence and Pressure Gradient on Local Skin Friction on Flat Plate. Ph.D. Thesis, Brown Univ., 1969.

8. Edwards, A.; and Furber, B. N.: The Influence of Free-Stream Turbulence on Heat Transfer by Convection from an Isolated Region of a Plane Surface in Parallel Air Flow. Proc. Inst. Mech. Eng., vol. 170, 1956, pp. 941-954.

9. Klein, John; and Tribus, Myron: Forced Convection from Nonisothermal Surfaces. Univ. Michigan Eng. Res. Inst., Aug. 1952. (Project M992-B, Contract AF 18(600)-51.)

NASA-Langley, 1973 —— 33 E-7165